and the indicated amount of geminin proteins. DNA (3 ng per μl of demembranated sperm chromatin) was added to the egg extract to start the reaction. After 90 min incubation at 23 °C, the reaction was stopped and the radioactivity incorporated into the acid-insoluble fraction was measured to quantify newly synthesized DNA. For a rescue experiment, 0.1 μM recombinant *Xenopus* Cdt1 was added to the reaction mixture that was used in replication inhibition assay.

Received 29 March; accepted 5 July 2004; doi:10.1038/nature02813.
Published online 1 August 2004.

1. Bell, S. P. & Dutta, A. DNA replication in eukaryotic cells. *Annu. Rev. Biochem.* **71,** 333–374 (2002).
2. Blow, J. J. & Hodgson, B. Replication licensing—defining the proliferative state? *Trends Cell Biol.* **12,** 72–78 (2002).
3. Diffley, J. F. DNA replication: building the perfect switch. *Curr. Biol.* **11,** R367–R370 (2001).
4. Bell, S. P. & Stillman, B. ATP-dependent recognition of eukaryotic origins of DNA replication by a multiprotein complex. *Nature* **357,** 128–134 (1992).
5. Coleman, T. R., Carpenter, P. B. & Dunphy, W. G. The *Xenopus* Cdc6 protein is essential for the initiation of a single round of DNA replication in cell-free extracts. *Cell* **87,** 53–63 (1996).
6. Nishitani, H., Lygerou, Z., Nishimoto, T. & Nurse, P. The Cdt1 protein is required to license DNA for replication in fission yeast. *Nature* **404,** 625–628 (2000).
7. Shreeram, S. & Blow, J. J. The role of the replication licensing system in cell proliferation and cancer. *Prog. Cell Cycle Res.* **5,** 287–293 (2003).
8. Vaziri, C. *et al.* A p53-dependent checkpoint pathway prevents rereplication. *Mol. Cell* **11,** 997–1008 (2003).
9. Kearsey, S. E. & Cotterill, S. Enigmatic variations: divergent modes of regulating eukaryotic DNA replication. *Mol. Cell* **12,** 1067–1075 (2003).
10. McGarry, T. J. & Kirschner, M. W. Geminin, an inhibitor of DNA replication, is degraded during mitosis. *Cell* **93,** 1043–1053 (1998).
11. Tada, S., Li, A., Maiorano, D., Mechali, M. & Blow, J. J. Repression of origin assembly in metaphase depends on inhibition of RLF-B/Cdt1 by geminin. *Nature Cell Biol.* **3,** 107–113 (2001).
12. Wohlschlegel, J. A. *et al.* Inhibition of eukaryotic DNA replication by geminin binding to Cdt1. *Science* **290,** 2309–2312 (2000).
13. Yamaguchi, R. & Newport, J. A role for Ran-GTP and Crm1 in blocking re-replication. *Cell* **113,** 115–125 (2003).
14. Li, A. & Blow, J. J. Non-proteolytic inactivation of geminin requires CDK-dependent ubiquitination. *Nature Cell Biol.* **6,** 260–267 (2004).
15. Hofmann, J. F. & Beach, D. Cdt1 is an essential target of the Cdc10/Sct1 transcription factor: requirement for DNA replication and inhibition of mitosis. *EMBO J.* **13,** 425–434 (1994).
16. Maiorano, D., Moreau, J. & Mechali, M. XCDT1 is required for the assembly of pre-replicative complexes in *Xenopus laevis*. *Nature* **404,** 622–625 (2000).
17. Whittaker, A. J., Royzman, I. & Orr-Weaver, T. L. *Drosophila* double parked: a conserved, essential replication protein that colocalizes with the origin recognition complex and links DNA replication with mitosis and the down-regulation of S phase transcripts. *Genes Dev.* **14,** 1765–1776 (2000).
18. Arentson, E. *et al.* Oncogenic potential of the DNA replication licensing protein CDT1. *Oncogene* **21,** 1150–1158 (2002).
19. Yanagi, K., Mizuno, T., You, Z. & Hanaoka, F. Mouse geminin inhibits not only Cdt1–MCM6 interactions but also a novel intrinsic Cdt1 DNA binding activity. *J. Biol. Chem.* **277,** 40871–40880 (2002).
20. Cook, J. G., Chasse, D. A. & Nevins, J. R. The regulated association of Cdt1 with minichromosome maintenance proteins and Cdc6 in mammalian cells. *J. Biol. Chem.* **279,** 9625–9633 (2004).
21. Bussiere, D. E., Bastia, D. & White, S. W. Crystal structure of the replication terminator protein from *B. subtilis* at 2.6 Å. *Cell* **80,** 651–660 (1995).
22. Gautam, A., Mulugu, S., Alexander, K. & Bastia, D. A single domain of the replication termination protein of *Bacillus subtilis* is involved in arresting both DnaB helicase and RNA polymerase. *J. Biol. Chem.* **276,** 23471–23479 (2001).
23. Tanaka, S. & Diffley, J. F. Interdependent nuclear accumulation of budding yeast Cdt1 and Mcm2–7 during G1 phase. *Nature Cell Biol.* **4,** 198–207 (2002).
24. O'Shea, E. K., Klemm, J. D., Kim, P. S. & Alber, T. X-ray structure of the GCN4 leucine zipper, a two-stranded, parallel coiled coil. *Science* **254,** 539–544 (1991).
25. Shreeram, S., Sparks, A., Lane, D. P. & Blow, J. J. Cell type-specific responses of human cells to inhibition of replication licensing. *Oncogene* **21,** 6624–6632 (2002).
26. Otwinowski, Z. & Minor, W. Processing of X-ray diffraction data collected in oscillation mode. *Methods Enzymol.* **276,** 307–326 (1997).
27. Brünger, A. T. *et al.* Crystallography and NMR system: A new software suite for macromolecular structure determination. *Acta Crystallogr. D* **54,** 905–921 (1998).
28. Kleywegt, G. J. & Jones, T. A. Efficient rebuilding of protein structures. *Acta Crystallogr. D* **50,** 829–832 (1996).
29. You, Z., Komamura, Y. & Ishimi, Y. Biochemical analysis of the intrinsic Mcm4–Mcm6–Mcm7 DNA helicase activity. *Mol. Cell. Biol.* **12,** 8003–8015 (1999).

Supplementary Information accompanies the paper on **www.nature.com/nature**.

Acknowledgements We thank S. Son and A. Jeon for help in initial protein purification, Y. Kong for MEF cells, J. Lee for anti-MCM6 antibody, and P. A. Karplus, S. H. Kim, Y. Kong and J. Bradbury for critical readings of the manuscript. This work was supported by the funds from the National Creative Research Initiatives (Ministry of Science and Technology).

Competing interests statement The authors declare that they have no competing financial interests.

Correspondence and requests for materials should be addressed to Y.C. (yunje@postech.ac.kr). The coordinates and structure factors have been deposited in the Protein Data Bank (accession code 1WLQ).

Structural basis for redox regulation of Yap1 transcription factor localization

Matthew J. Wood[1], Gisela Storz[1] & Nico Tjandra[2]

[1]*Cell Biology and Metabolism Branch, National Institute of Child Health and Human Development, National Institutes of Health, Bethesda, Maryland 20892-5430, USA*
[2]*Laboratory of Biophysical Chemistry, National Heart, Lung and Blood Institute, National Institutes of Health, Bethesda, Maryland 20892-8013, USA*

The ability of organisms to alter their gene expression patterns in response to environmental changes is essential for viability. A central regulator of the response to oxidative stress in *Saccharomyces cerevisiae* is the Yap1 transcription factor. Upon activation by increased levels of reactive oxygen species, Yap1 rapidly redistributes to the nucleus where it regulates the expression of up to 70 genes[1–3]. Here we identify a redox-regulated domain of

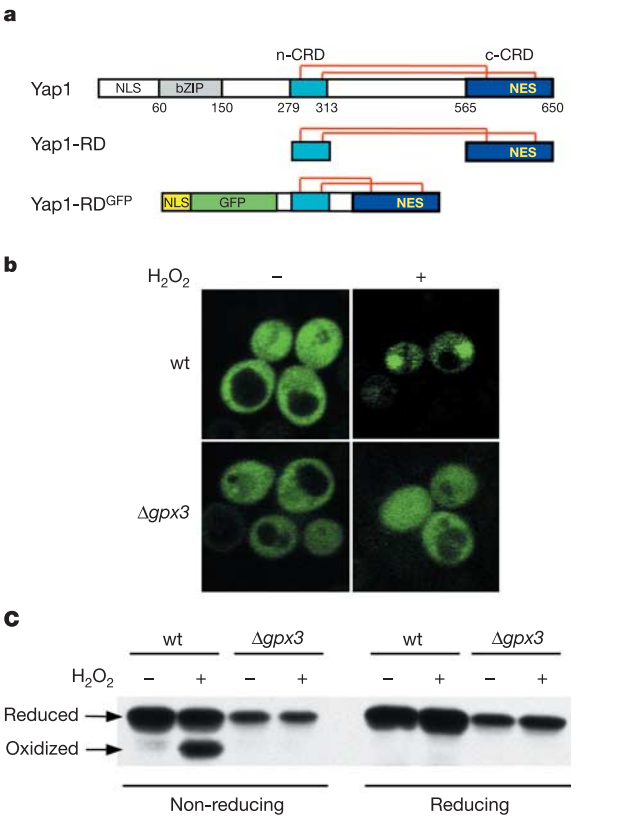

Figure 1 Schematic Yap1 structures and *in vivo* analysis of Yap1-RD^{GFP} subcellular localization and oxidation. **a**, Yap1 contains three conserved regions: a basic leucine zipper DNA binding domain (bZIP), an n-CRD (Asn279 to Arg313) and a c-CRD, (Asn565 to Asn650). The NLS and NES are located at the N and C termini, respectively. The Cys303–Cys598 and Cys310–Cys629 disulphide bonds are shown with red lines. The oxidized Yap1-RD construct used for structure determination consisted of the protease-resistant n-CRD and c-CRD domains. Yap1-RD^{GFP} consisted of an SV40 NLS, GFP and residues Asn279 to Arg313 fused to residues Asn549 to Asn650 of Yap1. This fragment encompasses the n-CRD and c-CRD sequences plus a small amount of the native linker. **b**, Fluorescence microscopy of wild-type and Δ*gpx3* cells expressing Yap1-RD^{GFP} from the native *YAP1* promoter on a *CEN* plasmid. **c**, Oxidized and reduced Yap1-RD^{GFP} extracted from wild-type and Δ*gpx3* cells. Exponentially growing cells were either exposed to H_2O_2 or left untreated. Cell extracts were run on non-reducing and reducing SDS–PAGE gels and probed with a GFP antibody.

Yap1 and determine its high-resolution solution structure. In the active oxidized form, a nuclear export signal (NES) in the carboxy-terminal cysteine-rich domain is masked by disulphide-bond-mediated interactions with a conserved amino-terminal α-helix. Point mutations that weaken the hydrophobic interactions between the N-terminal α-helix and the C-terminal NES-containing domain abolished redox-regulated changes in subcellular localization of Yap1. Upon reduction of the disulphide bonds, Yap1 undergoes a change to an unstructured conformation that exposes the NES and allows redistribution to the cytoplasm. These results reveal the structural basis of redox-dependent Yap1 localization and provide a previously unknown mechanism of transcription factor regulation by reversible intramolecular disulphide bond formation.

Yap1 regulates the transcription of antioxidant defence genes in response to reactive oxygen species such as H_2O_2. In unstressed cells, Yap1 is freely imported and exported from the nucleus[4,5]. In cells exposed to H_2O_2, nuclear export is arrested because Yap1 can no longer interact with the conserved nuclear exporter Crm1 (also known as Xpo1) (ref. 4). This redox control of Yap1 nuclear export requires an N-terminal cysteine-rich domain (n-CRD) and a C-terminal cysteine-rich domain (c-CRD), which encompasses the NES[1,6] (Fig. 1a).

The oxidized form of Yap1 contains a protease-resistant domain, Yap1-RD, comprised of residues Asn279 to Arg313 of the n-CRD and Asn565 to Asn650 of the c-CRD, covalently attached via Cys303–Cys598 and Cys310–Cys629 disulphide bonds[7] (Fig. 1a). To determine whether the subcellular localization of this domain is regulated like full-lengthYap1 in response to H_2O_2, we expressed a fusion protein containing a simian virus 40 (SV40) nuclear localization signal (NLS), green fluorescent protein (GFP) and Yap1-RD (hereafter referred to as Yap1-RD^{GFP}) in *S. cerevisiae* (Fig. 1a). In untreated cells Yap1-RD^{GFP} was localized throughout the cell (Fig. 1b). In cells treated with H_2O_2, Yap1-RD^{GFP} was relocalized to the nucleus within 5 min (Fig. 1b), as is the case with full-length Yap1 (refs 6, 8) (Supplementary Fig. S1). We also examined Yap1-RD^{GFP} localization in a Δ*gpx3* null strain. Gpx3 (also known as Orp1) has been shown to regulate Yap1 oxidation *in vivo*[9]. Like the full-length protein, Yap1-RD^{GFP} was no longer redistributed to the nucleus in a Δ*gpx3* strain treated with H_2O_2 (Fig. 1b). To confirm that Yap1-RD^{GFP} could be oxidized *in vivo*, we made cell extracts from wild-type and Δ*gpx3* strains treated with H_2O_2 or left untreated, and monitored the gel mobility of Yap1-RD^{GFP}. Upon treatment with H_2O_2, Yap1-RD^{GFP} migrated faster on non-reducing SDS–polyacrylamide gel electrophoresis (PAGE) gels, indicative of an oxidized form of the protein[8] (Fig. 1c). When these samples were run under reducing conditions the protein reverted back to a slower migrating species, indicative of the reduced form of the protein (Fig. 1c). Extracts prepared from a Δ*gpx3* strain showed no Yap1-RD^{GFP} oxidation upon H_2O_2 treatment (Fig. 1c). Thus the redox-dependent regulation of Yap1 could be reconstituted with Yap1-RD.

The ability to recast the redox regulation with Yap1-RD provided an opportunity for mechanistic and structural studies. To elucidate how the subcellular localization of Yap1 is controlled by reduction and oxidation, we determined the high resolution nuclear magnetic resonance (NMR) structure of oxidized Yap1-RD (Fig. 1a). The n-CRD contained a short eight-residue α-helix (n-α1), whereas the c-CRD contains both β-sheets and α-helices starting at Ser594 and continuing to residue Asn650 (Fig. 2b). Backbone amide ^{15}N relaxation measurements (T_2) also showed that ~70 amino acids in both the n-CRD and c-CRD are well ordered and that the structured regions correlate with areas of homology and secondary

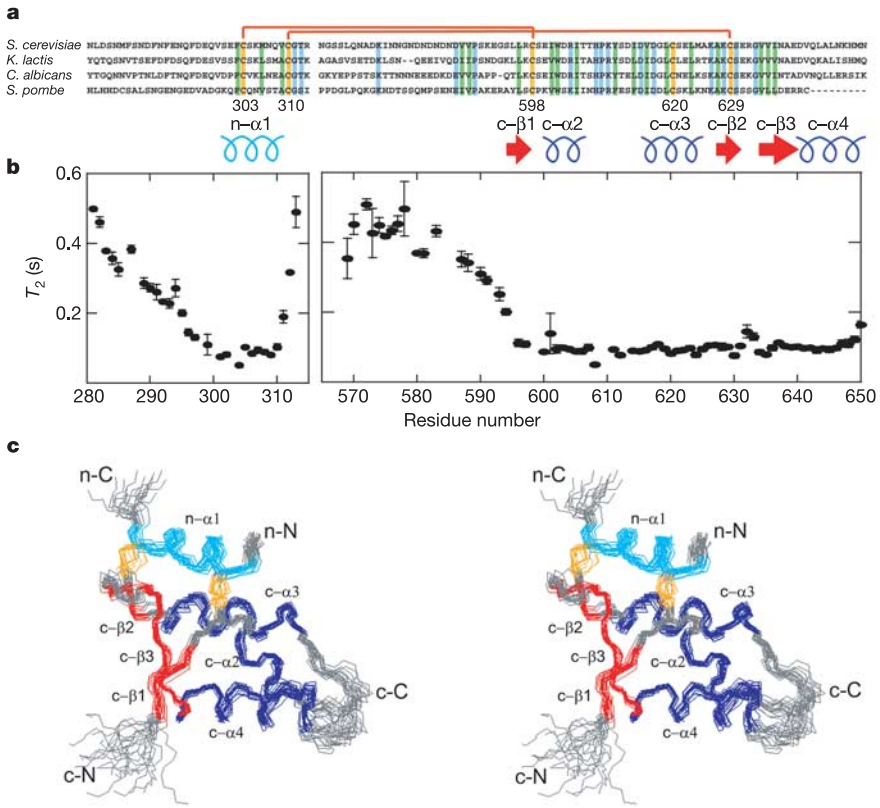

Figure 2 Structural characterization of oxidized Yap1-RD. **a**, Comparison of the n-CRD and c-CRD domains of four Yap1 homologues. The conserved cysteine and hydrophobic residues are highlighted in yellow and green, respectively. All other conserved residues are highlighted in blue. The Cys303–Cys598 and Cys310–Cys629 disulphide bonds are shown with red lines. **b**, The secondary structure and ^{15}N backbone dynamics (T_2) of Yap1-RD. Error bars indicate s.d. **c**, Stereo view of the backbone superposition of the ensemble of 20 Yap1-RD NMR structures with only the structured regions shown. n-CRD n-α1 helix, cyan; c-CRD β-sheets, red; c-CRD α-helices, dark blue; all other regions, grey. The Cys303–Cys598 and Cys310–Cys629 disulphide bonds are shown in yellow. The N and C termini of the n-CRD and c-CRD are indicated with an n- and c-, respectively.

structure (Fig. 2a, b). In addition, the $T_2^{average}$ for the structured regions of the n-CRD and c-CRD are the same, indicating that the two peptides comprising the structured regions of oxidized Yap1-RD behave as a single, well folded protein domain. The 20 lowest energy structures calculated for Yap1-RD have a backbone average r.m.s. deviation of 0.73 Å for the structured regions (Fig. 2c). Both the Cys303–Cys598 and Cys310–Cys629 disulphide bonds are on one side of the Yap1-RD structure, with the side chains of the disulphide-bonded cysteine residues largely solvent-exposed (Figs 2c and 3a).

The residues comprising the NES of Yap1-RD are located on the c-α3 helix and interact with conserved hydrophobic residues in the n-α1 helix (Fig. 3a, b). Previous experiments have shown that Leu619 is critically important for Yap1 nuclear export, whereas residues Ile614, Val616 and Leu623 are moderately important[4,8]. Both Leu619 and Leu623 are buried in the hydrophobic core of Yap1-RD and are completely solvent-inaccessible whereas Ile614 and Val616 are partially exposed (Fig. 3a, b). Importantly, the Val616, Leu619 and Leu623 side chains form extensive hydrophobic contacts with Phe302 and Met306 on the n-α1 helix (Fig. 3b, c). The phenyl ring of Phe302 locks Leu619 into the hydrophobic core and also interacts with Val616. The side chain of Met306 directly interacts with Leu623 and inserts into the central hydrophobic cavity of the c-CRD. In addition, Val309 interacts with the c-α3 helix, but is mostly solvent-exposed and has a modest number of contacts with Met624 and Ala627.

On the basis of the Yap1-RD structure, we proposed that point mutations of residues within the n-α1 helix would prevent the ability of Yap1 to oxidize and mask its NES. In particular, Phe302 and Met306 seemed to be critical for stabilization of the n-CRD and c-CRD interaction in the oxidized conformation (Fig. 3c). To test our hypothesis that the conserved hydrophobic residues on the n-α1 helix are critical for Yap1 function, we mutated Phe302, Met306 and Val309 to alanine and analysed Yap1-RD^{GFP} localization and redox state in response to H_2O_2. The F302A and M306A mutants both showed impaired nuclear accumulation and did not oxidize upon H_2O_2 treatment (Fig. 3d, e). In contrast, the V309A mutant showed a phenotype similar to wild-type Yap1-RD^{GFP} (Fig. 3d, e). The F302A and M306A mutants of full-length Yap1 also showed impaired nuclear accumulation and oxidation in response to H_2O_2 treatment, whereas the V309A mutant behaved in a similar way to the wild type (Supplementary Fig. S1). These results show that disulphide bonds are not enough to stabilize the interaction between the n-CRD and the c-CRD, and suggest that masking of the NES requires specific interactions involving both Phe302 and Met306. It is also possible that the Phe302 and Met306 mutations affect the redox potential of the Cys303 and Cys310 residues.

To understand how the reduction of oxidized Yap1 results in unmasking of the NES and redistribution of the protein to the cytoplasm, we treated a ^{15}N-labelled sample of oxidized Yap1-RD with the reducing agent dithiothreitol (DTT) and monitored changes in its ^{1}H and ^{15}N chemical shifts with NMR. Upon reduction, the peaks assigned to structured residues of Yap1-RD completely disappeared and the ^{1}H–^{15}N hetero-nuclear single quantum coherence (HSQC) spectrum was characteristic of a protein with little secondary and tertiary structure[10] (Fig. 4a). A comparison of the circular dichroism spectra of oxidized and reduced Yap1-RD also showed a loss of secondary structure upon reduction with DTT (Fig. 4b). Furthermore, size exclusion chromatography indicated that upon reduction, the n-CRD and c-CRD peptides dissociate and migrate separately at molecular weights characteristic of unfolded peptides (data not shown). Biophysical studies using oxidized full-length Yap1 also show conformational changes upon reduction with DTT (ref. 7). Although we cannot rule out the possibility that the c-CRD may adopt a structured conformation in the reduced form as a result of interactions with other

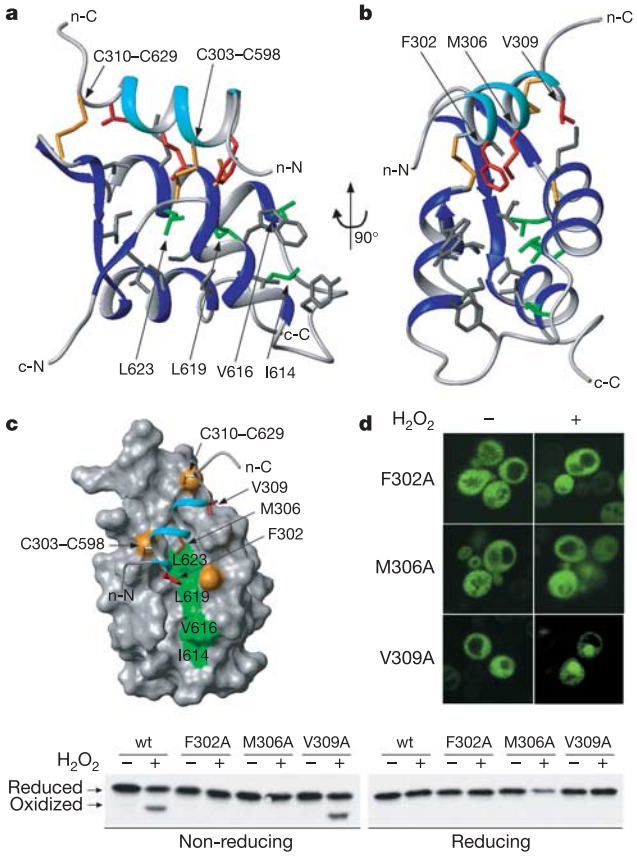

Figure 3 Inhibition of the Yap1 NES by the n-α1 helix. **a**, Ribbon diagram of the Yap1-RD structure with the lowest energy shown in the same orientation as Fig. 2c. The n-α1 helix and the regions of c-CRD secondary structure are shown in cyan and dark blue, respectively. The NES residues Ile614, Val616, Leu619 and Leu623 are shown in green. These interact with other hydrophobic core residues of the c-CRD, which are shown in grey. **b**, The same ribbon diagram as in Fig. 3a, rotated to show the n-α1 residues. The amphipathic n-α1 helix contains conserved hydrophobic residues, Phe302, Met306 and Val309, shown in red. **c**, Surface representation of the c-CRD domain and its interaction with the hydrophobic residues in the n-α1 helix. The surface of the NES residues Ile614, Val616, Leu619 and Leu623 are shown in green and Phe302, Met306 and Val309 in red. **d**, Fluorescence microscopy of cells expressing Yap1-RD^{GFP} F302A, M306A and V309A mutants, untreated or treated with H_2O_2 as carried out in Fig. 1b. **e**, Oxidized and reduced Yap1-RD^{GFP} F302A, M306A and V309A mutants extracted from exponentially growing cells untreated or treated with H_2O_2. The cell extracts were prepared as in Fig. 1c.

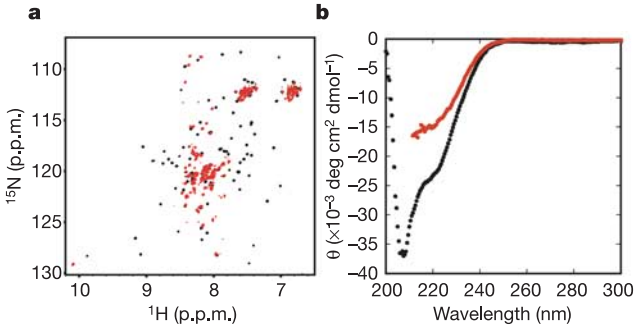

Figure 4 Redox-mediated conformational changes in Yap1-RD. **a**, HSQC spectra of ^{15}N-labelled oxidized (black) and reduced (red) Yap1-RD. Yap1-RD was reduced by the addition of 20 mM DTT for 10 min before collecting an HSQC spectrum. **b**, Circular dichroism spectra of oxidized (black) and reduced (red) Yap1-RD. All circular dichroism experiments were performed with a 0.1-cm-pathlength cell and 30 μM Yap1-RD prepared in the same way as the NMR samples.

proteins or portions of Yap1 that are not present in Yap1-RD, our observations suggest that in reduced Yap1 the NES is exposed, allowing Yap1 to be exported from the nucleus by Crm1. Upon oxidation, Yap1 adopts a conformation in which the NES is concealed, as indicated in this structure, allowing Yap1 to accumulate in the nucleus.

To our knowledge, the oxidized Yap1-RD structure is the first known high resolution structure of the sensory domain of a eukaryotic transcription factor that is reversibly regulated by disulphide bond formation. Comparison of Yap1 with other redox-regulated proteins indicates that redox-mediated conformational changes are a general mechanism for regulation of protein function. The formation of a single disulphide bond in OxyR, a transcription factor in *Escherichia coli*, results in restructuring of the protein, leading to a change in DNA binding[11]. The domain containing the redox active cysteines in the *E. coli* heat shock protein Hsp33 becomes more flexible upon oxidation, allowing association of the Hsp33 dimerization domains and subsequent activation of the chaperone[12,13]. An intriguing aspect of Yap1 regulation is that the disulphide-bonded cysteine residues are separated by a large ~300-amino-acid flexible domain. The mechanism by which the distant n-CRD and c-CRD domains are rapidly and precisely brought together remains to be determined.

Control of subcellular localization is a well established theme in the regulation of eukaryotic transcription factors[14,15]. As far as we know, the Yap1 structure is the first example of NES masking mediated by intramolecular disulphide bonds. Other mechanisms by which protein localization signals are masked include phosphorylation of the NLS sequences of NF-AT transcription factors and oligomerization and burial of the NES of the p53 transcription factor[16–18]. In addition, the dileucine protein-sorting motif of CD4 is masked when it is in a complex with the protein Lck and Zn^{2+}, whereas uncomplexed CD4 is unstructured and the dileucine protein sorting motif is exposed[19]. We suggest that redox-controlled masking of a signal sequence may represent a general stress-sensitive mechanism for controlling accessibility of protein localization signals. □

Methods

Plasmids, strains and growth conditions

The *S. cerevisiae* parent strain used in this study is YPH499 (*MAT***a** *ura3-52 lys2-801*^{amber} *ade2-101*^{ochre} *trp1-Δ63 his3-Δ200 leu2-Δ1*). The isogenic Δ*gpx3* derivative was made by replacing the coding region of *GPX3* with KanMX (ref. 20). The Yap1-RD-expressing plasmid was made by separate PCR amplifications of the sequences comprising Asn279 to Lys327 (n-CRD) and Gln549 to Asn650 (c-CRD) of Yap1. These PCR reactions were ligated into the pRSET expression vector (Invitrogen). The Yap1-RD expression construct does not code for any non-native amino acids between the n-CRD and c-CRD. The Yap1-RD^{GFP} plasmid was constructed by subcloning PCR fragments comprised of the *YAP1* promoter and SV40 NLS, enhanced GFP, Yap1-RD and *CYC1* terminator into the pRS316 yeast *CEN* vector (primer sequences available on request)[20]. Yap1-RD^{GFP} n-CRD point mutants were made using standard oligonucleotide PCR-based mutagenesis procedures. All yeast strains were grown at 30 °C in minimal media containing 0.67% (w/v) yeast nitrogen bases, 2% (w/v) glucose and amino-acid dropout mix supplemented with adenine.

Fluorescence microscopy

Exponentially growing cells carrying Yap1-RD^{GFP} constructs were treated with H_2O_2 for 10 min and analysed with a confocal microscope system (model LSM 510; Carl Zeiss MicroImaging, Inc.) using the 488-nm line.

Preparation of cell extracts

Cell extracts were prepared from exponentially growing cells carrying the Yap1-RD^{GFP} constructs. The cells were treated with H_2O_2 for 5 min and prepared as previously described[8]. Yap1-RD^{GFP} samples were run on 8% SDS–PAGE gels, transferred to nitrocellulose and probed with anti-GFP monoclonal antibodies (Roche Applied Science).

Preparation of Yap1-RD

Yap1-RD was expressed in *E. coli*, purified on Ni-NTA (Qiagen) and Mono-Q (Amersham Pharmacia) columns and oxidized as previously described[7]. Oxidized Yap1-RD was digested with a limiting amount of trypsin for 5 h and purified using reverse phase high-performance liquid chromatography. After digestion and purification, the masses of the n-CRD and c-CRD peptides comprising Yap1-RD showed that they consisted of Yap1 residues Asn279 to Arg313 and Asn565 to Asn650, respectively. The Cys303–Cys598 and Cys310–Cys629 disulphide-bonding pattern of Yap1-RD was confirmed using matrix-assisted laser desorption/ionization mass spectrometry. Isotopically labelled proteins were prepared from cells grown in minimal media containing $^{15}NH_4Cl$ and unlabelled or ^{13}C-labelled glucose[21].

NMR spectroscopy

NMR data were acquired on Bruker 600- and 800-MHz spectrometers equipped with triple resonance probes or a cryoprobe. All experiments were performed with ~0.8 mM Yap1-RD at 303 K in 10 mM sodium phosphate (pH 6.0), containing 20 mM NaCl and 10% ^2H_2O. All spectra were processed with NMRPipe and analysed with PIPP (refs 22, 23). We obtained backbone resonance assignment using standard triple-resonance experiments[24]. Four-dimensional $^{15}N/^{13}C$-edited and $^{13}C/^{13}C$-edited nuclear Överhauser enhancement (NOE) experiments were used to obtain NOE assignments and distance restraints[24]. The presence of disulphide bonds was confirmed by the observation of numerous contacts between Cys303 and Cys598 as well as Cys310 and Cys629. No contacts to other cysteine residues were observed for Cys620. The $^{13}C_\beta$ chemical shifts for Cys303, Cys310, Cys598 and Cys629 were consistent with oxidized cysteines and the $^{13}C_\beta$ chemical shift of Cys620 was consistent with a reduced cysteine[25]. The TALOS program was used to obtain phi and psi backbone dihedral restraints[26]. NMR experiments to measure residual dipolar couplings were performed on phage-containing samples[27].

Structure calculations

Peak intensities from nuclear Överhauser enhancement spectroscopy experiments were translated into a continuous distribution of interproton distances. Structures of Yap1-RD were calculated by a distance geometry and simulated annealing protocol with the incorporation of $^{15}N–^1H$ and $^{13}C_\alpha–^1H$ dipolar coupling restraints using XPLOR-NIH (refs 28, 29). Structural statistics for the ensemble of 20 Yap1-RD structures are listed in Supplementary Table 1.

Received 24 March; accepted 28 June 2004; doi:10.1038/nature02790.

1. Kuge, S., Jones, N. & Nomoto, A. Regulation of yAP-1 nuclear localization in response to oxidative stress. *EMBO J.* **16,** 1710–1720 (1997).
2. Godon, C. *et al.* The H_2O_2 stimulon in *Saccharomyces cerevisiae*. *J. Biol. Chem.* **273,** 22480–22489 (1998).
3. Gasch, A. P. *et al.* Genomic expression programs in the response of yeast cells to environmental changes. *Mol. Biol. Cell* **11,** 4241–4257 (2000).
4. Yan, C., Lee, L. H. & Davis, L. I. Crm1p mediates regulated nuclear export of a yeast AP-1-like transcription factor. *EMBO J.* **17,** 7416–7429 (1998).
5. Isoyama, T., Murayama, A., Nomoto, A. & Kuge, S. Nuclear import of the yeast AP-1-like transcription factor Yap1p is mediated by transport receptor Pse1p, and this import step is not affected by oxidative stress. *J. Biol. Chem.* **276,** 21863–21869 (2001).
6. Coleman, S. T., Epping, E. A., Steggerda, S. M. & Moye-Rowley, W. S. Yap1p activates gene transcription in an oxidant-specific fashion. *Mol. Cell. Biol.* **19,** 8302–8313 (1999).
7. Wood, M. J., Andrade, E. C. & Storz, G. The redox domain of the Yap1p transcription factor contains two disulfide bonds. *Biochemistry* **42,** 11982–11991 (2003).
8. Delaunay, A., Isnard, A. D. & Toledano, M. B. H_2O_2 sensing through oxidation of the Yap1 transcription factor. *EMBO J.* **19,** 5157–5166 (2000).
9. Delaunay, A., Pflieger, D., Barrault, M. B., Vinh, J. & Toledano, M. B. A thiol peroxidase is an H_2O_2 receptor and redox-transducer in gene activation. *Cell* **111,** 471–481 (2002).
10. Demarest, S. J. *et al.* Mutual synergistic folding in recruitment of CBP/p300 by p160 nuclear receptor coactivators. *Nature* **415,** 549–553 (2002).
11. Choi, H. *et al.* Structural basis of the redox switch in the OxyR transcription factor. *Cell* **105,** 103–113 (2001).
12. Graumann, J. *et al.* Activation of the redox-regulated molecular chaperone Hsp33–a two-step mechanism. *Structure (Camb)* **9,** 377–387 (2001).
13. Vijayalakshmi, J., Mukhergee, M. K., Graumann, J., Jakob, U. & Saper, M. A. The 2.2 A crystal structure of Hsp33: a heat shock protein with redox-regulated chaperone activity. *Structure (Camb)* **9,** 367–375 (2001).
14. Kaffman, A. & O'Shea, E. K. Regulation of nuclear localization: a key to a door. *Annu. Rev. Cell Dev. Biol.* **15,** 291–339 (1999).
15. Kau, T. R., Way, J. C. & Silver, P. A. Nuclear transport and cancer: from mechanism to intervention. *Nature Rev. Cancer* **4,** 106–117 (2004).
16. Zhu, J. *et al.* Intramolecular masking of nuclear import signal on NF-AT4 by casein kinase I and MEKK1. *Cell* **93,** 851–861 (1998).
17. Clore, G. M. *et al.* High-resolution structure of the oligomerization domain of p53 by multidimensional NMR. *Science* **265,** 386–391 (1994).
18. Stommel, J. M. *et al.* A leucine-rich nuclear export signal in the p53 tetramerization domain: regulation of subcellular localization and p53 activity by NES masking. *EMBO J.* **18,** 1660–1672 (1999).
19. Kim, P. W., Sun, Z. Y., Blacklow, S. C., Wagner, G. & Eck, M. J. A zinc clasp structure tethers Lck to T cell coreceptors CD4 and CD8. *Science* **301,** 1725–1728 (2003).
20. Sikorski, R. S. & Hieter, P. A system of shuttle vectors and yeast host strains designed for efficient manipulation of DNA in *Saccharomyces cerevisiae*. *Genetics* **122,** 19–27 (1989).
21. Suzuki, M., Youle, R. J. & Tjandra, N. Structure of Bax: coregulation of dimer formation and intracellular localization. *Cell* **103,** 645–654 (2000).
22. Delaglio, F. *et al.* NMRPipe: a multidimensional spectral processing system based on UNIX pipes. *J. Biomol. NMR* **6,** 277–293 (1995).
23. Garrett, D. S., Powers, R., Gronenborn, A. M. & Clore, G. M. A common-sense approach to peak picking in 2-dimensional, 3-dimensional, and 4-dimensional spectra using automatic computer-analysis of contour diagrams. *J. Magn. Reson.* **95,** 214–220 (1991).
24. Clore, G. M. & Gronenborn, A. M. Multidimensional heteronuclear nuclear magnetic resonance of proteins. *Methods Enzymol.* **239,** 349–363 (1994).
25. Cavanagh, J., Fairbrother, W. J., Palmer, A. G. & Skelton, N. J. *Protein NMR Spectroscopy: Principles and Practice* (Academic, San Diego, 1995).

26. Cornilescu, G., Delaglio, F. & Bax, A. Protein backbone angle restraints from searching a database for chemical shift and sequence homology. *J. Biomol. NMR* **13,** 289–302 (1999).
27. Hansen, M. R., Mueller, L. & Pardi, A. Tunable alignment of macromolecules by filamentous phage yields dipolar coupling interactions. *Nature Struct. Biol.* **5,** 1065–1074 (1998).
28. Tjandra, N., Omichinski, J. G., Gronenborn, A. M., Clore, G. M. & Bax, A. Use of dipolar $^{1}H–^{15}N$ and $^{1}H–^{13}C$ couplings in the structure determination of magnetically oriented macromolecules in solution. *Nature Struct. Biol.* **4,** 732–738 (1997).
29. Schwieters, C. D., Kuszewski, J. J., Tjandra, N. & Clore, G. M. The Xplor-NIH NMR molecular structure determination package. *J. Magn. Reson.* **160,** 65–73 (2003).

Supplementary Information accompanies the paper on **www.nature.com/nature**.

Acknowledgements We would like to thank E. Andrade for preparing the Yap1-RD expression construct, S. Moye-Rowley for providing reagents, C. Jackson for suggestions, C. Wu for use of the mass spectrometer and C. A. Combs for his expertise and advice regarding microscopy-related experiments. We also thank A. Gronenborn, R. Hegde, E. Komives, E. Korn, S. Moye-Rowley and W. Outten for critical reading of this manuscript. M.J.W. is supported by a Research Associateship from the National Research Council.

Competing interests statement The authors declare that they have no competing financial interests.

Correspondence and requests for materials should be addressed to G.S. (storzg@mail.nih.gov) or N.T. (nico@helix.nih.gov). Yap1-RD coordinates have been deposited with the Protein Data Bank under accession number 1SSE.

erratum

No stellar p-mode oscillations in space-based photometry of Procyon

Jaymie M. Matthews, Rainer Kuschnig, David B. Guenther, Gordon A. H. Walker, Anthony F.J. Moffat, Slavek M. Rucinski, Dimitar Sasselov & Werner W. Weiss

Nature **430,** 51–53 (2004).

In this Letter, Rainer Kuschnig's surname was misspelled as 'Kusching' in the author list. In addition, the numbering of the reference list was incorrect. References 1 to 26 should be, respectively: 1, 10–16, 2, 3, 17–26 and 4–9. In ref. 23 (ref. 6), 'Rettler' should read 'Retter'. □

corrigendum

Sirt1 promotes fat mobilization in white adipocytes by repressing PPAR-γ

Frédéric Picard, Martin Kurtev, Namjin Chung, Acharawan Topark-Ngarm, Thanaset Senawong, Rita Machado de Oliveira, Mark Leid, Michael W. McBurney & Leonard Guarente

Nature **429,** 771–776 (2004).

It has been drawn to our attention by Vincent Keng that the image in the bottom-left frame of Fig. 1c of this Letter presents identical data to the one above it on the right. A mistake made by the authors during compilation of Fig.1 caused the wrong bottom-left image to be used instead of the correct image, which is shown below. The results presented in this replacement micrograph do not alter the conclusions of our study. □